Tips for Quick Calculation and Deciphering of Radiation Spectra

M.V. Bondarenco

NSC Kharkov Institute of Physics & Technology, Kharkov, Ukraine
V.N. Karazine Kharkov National University, Kharkov, Ukraine

September 20, 2017, RREPS-2017, DESY, Hamburg, Germany

Contents

Introduction

The relation between motions of fast electrons and the corresponding radiation spectra in general is rather complicated. In a finite target, it is further encumbered by an interplay of volume and edge effects [1, 2], which can be separated according to diagram 1 (see [2] for discussion). But certain simplifications can arise away from the boundary lines, where it may be possible to reduce the double time integral to a single one.

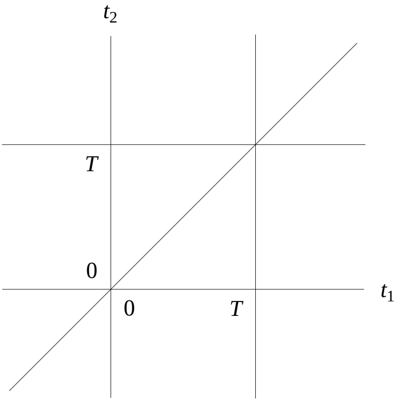

Figure: Domains of continuity of the integrand of the double time integral for the radiation spectrum.

Infrared asymptotics up to NLO ($I_f(\omega) \gg T$)

For instance, the well-known infrared factorization theorem [3, 4] states that the limiting value of the spectrum at $\omega \to 0$ depends solely on the final electron deflection angle, viz.,

$$\frac{dI_{\rm BH}}{d\omega} = \frac{e^2}{(2\pi)^2}\int d^2n \left| \frac{\vec{n}\times\vec{v}_f(t)}{1-\vec{n}\cdot\vec{v}_f(t)} - \frac{\vec{n}\times\vec{v}_i(t)}{1-\vec{n}\cdot\vec{v}_i(t)} \right|^2 = \frac{2e^2}{\pi}\left(\frac{2+\gamma^2 v_{fi}^2}{\gamma v_{fi}\sqrt{1+\gamma^2 v_{fi}^2/4}} \operatorname{arsinh}\frac{\gamma v_{fi}}{2} - 1 \right). \tag{1}$$

The merit of formula (1) is its independence of the detail of electron motion inside the target. To predict behavior of the spectrum for all ω, one often interpolates between (1) and the result found in the approximation of a “thick” target (see the next section). But to this end, it may be expedient also to find a correction to (1):

$$\frac{dI}{d\omega} \underset{\omega\to 0}{\simeq} \frac{dI_{\rm BH}}{d\omega} + C_1\omega + \mathcal{O}\left(\omega^2\right), \tag{2}$$

with [5]

$$C_1 = -\frac{e^2}{2}\int_{-\infty}^{\infty} dt[\vec{v}(t)-\vec{v}_i]\cdot[\vec{v}_f-\vec{v}(t)]. \tag{3}$$

(In contrast to the Low theorem [6], C_1 does *not* express through the scattering characteristics.) Physically, correction $C_1\omega$ is related to a difference between the time delay $v\tau - \left|\vec{r}(\tau)-\vec{r}(0)\right|$ for the actual trajectory and for its angle-shaped approximation.

For monotonous electron deflection, $C_1 < 0$ (see Fig. 2);
for amorphous target, $C_1 = 0$;
for an oscillatory motion within the target, $C_1 > 0$.
For example, in case of undulator radiation, when $\vec{F}_\perp(t) = \vec{F}_0 \cos\frac{2\pi t}{T_1}$ within the interval $0 < t < NT_1$, where $N \gg 1$ is the number of oscillation periods,

$$\frac{C_1}{NT_1} \underset{N\to\infty}{\simeq} e^2 \left(\frac{F_0 T_1}{4\pi E}\right)^2 . \tag{4}$$

At application of result (3), it is worth minding that it is insensitive to non-dipole radiation effects. Thus, relation (4), well known for dipole undulators, must equally well hold for wigglers.

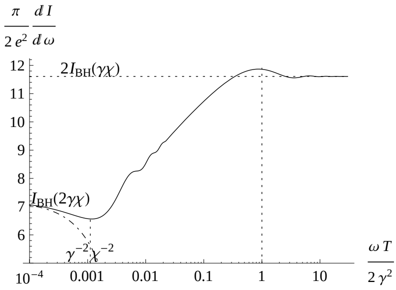

Figure: Spectrum of radiation at double scattering of an electron through two equal angles $\vec{\chi}_1 = \vec{\chi}_2$ [2]. Due to the negative $C_1 = -\frac{e^2}{2}\vec{\chi}_1 \cdot \vec{\chi}_2 t_{21}$, the spectrum appears to be non-monotonous at low ω.

Radiation in thick targets ($T \gg l_f(\omega)$). Quick averaging

In thick targets, when most of the photons are generated deeply inside the target, one may merely neglect edge effects and deal with the radiation yield per unit time:

$$\frac{dI}{d\omega dt} = \omega \frac{e^2}{\pi} \int_0^\infty \frac{d\tau}{\tau} \left\{ \left(\gamma^{-2} + \frac{1}{2} \left[\vec{v}(\tau) - \vec{v}(0) \right]^2 \right) \sin \omega \left[\tau - \left| \vec{r}(\tau) - \vec{r}(0) \right| \right] - \gamma^{-2} \sin \omega (1 - v) \tau \right\}, \quad (5)$$

where the argument of the first sine can be related to the prefactor:

$$v\tau - |\vec{r}(\tau) - \vec{r}(0)| \simeq \frac{v}{2\tau} \int_0^\tau ds_2 \int_0^{s_2} ds_1 \left[\vec{v}(s_2) - \vec{v}(s_1) \right]^2 . \quad (6)$$

With the account of averaging, to avoid multiple integrals, one may replace $\left[\vec{v}(\tau) - \vec{v}(0) \right]^2$ and (6) by their averages and heuristically insert them to (5). This approach was devised by Landau and Pomeranchuk in their pioneering paper on LPM effect [7]. Admittedly, it is not quite correct, but is attractive by its simplicity, so one may be interested how accurate it can be in practice. In the dipole limit, it tends to the exact result, so the only question is about its validity in the opposite, synchrotron-like regime. Let us consider two examples.

Radiation in an amorphous target

With $\left[\vec{v}(\tau)-\vec{v}(0)\right]^2=\left\langle\frac{d\chi^2}{d\tau}\right\rangle\tau$, $v\tau-|\vec{r}(\tau)-\vec{r}(0)|=\frac{1}{12}\left\langle\frac{d\chi^2}{d\tau}\right\rangle\tau^2$, we get

$$\frac{dI}{d\omega dt} = \omega\frac{e^2}{\pi}\int_0^\infty\frac{d\tau}{\tau}\left\{\left(\gamma^{-2}+\frac{1}{2}\left\langle\frac{d\chi^2}{d\tau}\right\rangle\tau\right)\sin\omega\left[(1-v)\tau+\frac{1}{12}\left\langle\frac{d\chi^2}{d\tau}\right\rangle\tau^2\right] -\gamma^{-2}\sin\omega(1-v)\tau\right\} \quad (7)$$

$$= \frac{dI_{BH}}{d\omega dt}\tilde{\Phi}\left(\frac{3\omega}{\gamma^4\left\langle\frac{d\chi^2}{d\tau}\right\rangle}\right), \quad (8)$$

where $\frac{dI_{BH}}{d\omega dt}=\frac{2e^2}{3\pi}\gamma^2\left\langle\frac{d\chi^2}{d\tau}\right\rangle$, while the formfactor reads

$$\tilde{\Phi}(\Omega_a)=\frac{9}{8}-\frac{\pi\Omega_a}{4}\left[S\left(\sqrt{\frac{\Omega_a}{2\pi}}\right)+\frac{3}{\sqrt{2\pi\Omega_a}}\cos\frac{\Omega_a}{4}-\frac{1}{2}\right]^2 -\frac{\pi\Omega_a}{4}\left[C\left(\sqrt{\frac{\Omega_a}{2\pi}}\right)-\frac{3}{\sqrt{2\pi\Omega_a}}\sin\frac{\Omega_a}{4}-\frac{1}{2}\right]^2, \quad (9)$$

with $C(z)=\int_0^z dt\cos\frac{\pi t^2}{2}$ and $S(z)=\int_0^z dt\sin\frac{\pi t^2}{2}$ being Fresnel integrals.

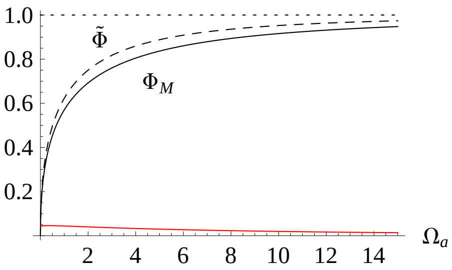

Figure: Comparison of (9) (dashed curve) with Migdal's function $\Phi_M\left(\frac{1}{4}\sqrt{\frac{\Omega_a}{3}}\right)$, $\Phi_M(s) = 6s^2\left\{4\mathfrak{Im}\,\psi[(1+i)s] - \frac{1}{s} - \pi\right\}$ (solid curve). The red line shows the relative difference $\frac{\tilde{\Phi}-\Phi_M}{\tilde{\Phi}+\Phi_M}$.

At $\Omega_a \to \infty$, $\tilde{\Phi} \to 1$, thus satisfying the Bethe-Heitler limit. That is natural because it corresponds to the dipole regime.

On the other hand, in the infrared limit $\Omega_a \to 0$, $\tilde{\Phi} \simeq \frac{3}{4}\sqrt{\frac{\pi\Omega_a}{2}}$. Compared to the correct asymptotic behavior known from the Migdal's theory $\Phi_M \simeq \frac{\sqrt{3\Omega_a}}{2}$, it differs by factor of $\sqrt{\frac{3\pi}{8}} = 1.085$, but in practice such a difference may often be regarded as small (see Fig. 3).

Radiation at doughnut scattering

A similar but more intricate problem is radiation at electron scattering on a family of aligned atomic strings (doughnut scattering). Assuming strings to be parallel but distributed randomly in the transverse plane, the kinetics of electron multiple scattering on them may be described by Focker-Plank equation

$$\frac{\partial f}{\partial \tau} = D\frac{\partial^2 f}{\partial \phi^2}, \qquad (10)$$

where ϕ is the azimuthal angle between velocity vectors relative to the string axis. Solving it with the initial condition $f(\phi, \vec{r}_\perp, 0) = \delta(\phi)\delta(\vec{r}_\perp)$, one finds

$$\left\langle [\mathbf{v}_\perp(\tau) - \mathbf{v}_\perp(0)]^2 \right\rangle = 2v_\perp^2 \left\langle 1 - \cos\phi \right\rangle = 2v_\perp^2(1 - e^{-D\tau}). \qquad (11)$$

$$\begin{aligned} v\tau - \left|\vec{r}(\tau) - \vec{r}(0)\right| &= \frac{v_\perp^2}{\tau}\int_0^\tau ds_2 \int_0^{s_2} ds_1 \left[1 - e^{-D(s_2 - s_1)}\right] \\ &= \frac{v_\perp^2}{D^2\tau}\left(1 - D\tau + \frac{D^2\tau^2}{2} - e^{-D\tau}\right). \end{aligned} \qquad (12)$$

The behavior of the spectrum obtained by plugging (11), (12) to (5) is shown in Fig. 4. It is in fair agreement with experimental data of [8].

Let us now scrutinize the accuracy of this approach at $\gamma v_\perp \gtrsim 1$. First of all, note that it interpolates smoothly between infrared and ultraviolet limits, and examine the spectrum behavior in those limits.

In the ultraviolet limit,

$$\frac{dI}{d\omega dt} \underset{\Omega_d \gg 1}{\simeq} \frac{4e^2\gamma^2 D}{3\pi} v_\perp^2$$

(essentially, a dipole behavior).

In the infrared limit,

$$\frac{dI}{d\omega dt} \underset{\Omega_d \ll 1}{\simeq} \frac{e^2\omega}{2} v_\perp^2,$$

which is $\propto v_\perp^2$, too! Thus, in the latter limit it must be exact under averaging, as well.

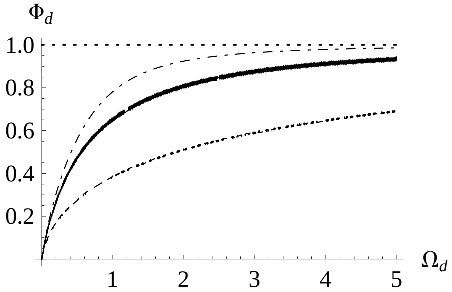

Figure: Behavior of formfactor $\Phi_d = \frac{3\pi}{4e^2\gamma^2 v_\perp^2 D}\frac{dI}{d\omega dt}$ evaluated by Eqs. (11), (12), (5).
Dot-dashed curve, $\gamma v_\perp \to 0$ [Eq. (13)].
Solid curve, $\gamma v_\perp = 1$. Dashed, $\gamma v_\perp = 3$.

To trace the overall spectral behavior, note that at $\gamma v_\perp \to 0$, it tends to the exact result

$$\frac{dI}{d\omega dt} \simeq \frac{4e^2\gamma^2}{3\pi v_\perp^2 D}\Phi_{d0}\left(\frac{\omega}{2D\gamma^2}\right),$$

$$\Phi_{d0}(\Omega_d) = \frac{3\Omega_d}{2}\left\{(1-2\Omega_d^2)\mathrm{arccot}\Omega_d + \Omega_d\left[2-\ln(1+\Omega_d^{-2})\right]\right\}. \qquad (13)$$

On the other hand, at $\gamma v_\perp \to \infty$, it tends to $\tilde{\Phi}(3\Omega_d/\gamma^2 v_\perp^2)$ where $\tilde{\Phi}$ given by Eq. (9) is attested to be a sustainable approximation in the region of its validity. At $\gamma v_\perp \sim 1$, it goes somewhere in between (see Fig. 4). Since it works well in both extremes and interpolates smoothly between them, it may happen to be numerically acceptable everywhere, thus offering a tenable simple theory of radiation at doughnut scattering.

Scaling in uniform media

Asymptotic behavior of radiation spectra at $\omega \to 0$ and $\omega \to \infty$ is usually related to behavior of correlators $\left[\vec{v}(\tau) - \vec{v}(0)\right]^2$ and $v\tau - \left|\vec{r}(\tau) - \vec{r}(0)\right|$ correspondingly at $\tau \to \infty$ and $\tau \to 0$. Let us analyze this relation on general grounds.

Assume a scaling property of particle motion (in the uniform medium):

$$\left[\vec{v}(\tau) - \vec{v}(0)\right]^2 = c_v \tau^n. \tag{14}$$

Substitution thereof to Eq. (6) yields

$$v\tau - \left|\vec{r}(\tau) - \vec{r}(0)\right| = \frac{c_v}{2\tau} \int_0^\tau ds_2 \int_0^{s_2} ds_1 \left(s_2 - s_1\right)^n = c_r \tau^{n+1}, \tag{15}$$

with

$$c_r = \frac{c_v}{2(n+1)(n+2)}.$$

For synchrotron radiation $n = 2$, whereas for LPM effect $n = 1$. For doughnut scattering, $n \simeq 1$ for $t \ll D$, and $n \to 0$ for $t \gg D$.

LO and NLO IR and UV asymptotics

Employing those items in integral (5), one can derive asymptotic expansion of the spectrum in the limit $\omega \to 0$:

$$\frac{dI}{d\omega dt} \underset{\omega\to 0}{\simeq} \frac{e^2 \sin\frac{\pi n}{2(n+1)}}{2\pi(n+1)} \Gamma\left(\frac{n}{n+1}\right) \frac{c_v \omega^{\frac{1}{n+1}}}{c_r^{\frac{n}{n+1}}} - \frac{e^2\omega}{2\gamma^2}\frac{n}{n+1} + \mathcal{O}(\omega^2). \tag{16}$$

Its LO term is independent of γ, thus being intrinsically radiophysical (see [2]). As for the NLO term, it proves to be independent of the strength of the force acting on the particle, and thus is the same for targets from different materials (e.g., Si and Ge crystals in the same orientation, or amorphous Al and Au, etc.).

In the UV limit, the asymptotics reads

$$\frac{dI}{d\omega dt} \underset{\omega\to\infty}{\simeq} \frac{e^2\gamma^2}{\pi}(c_v - 4nc_r)\left(\frac{2\gamma^2}{\omega}\right)^{n-1} \Gamma(n)\sin\frac{\pi n}{2} + \frac{e^2}{2\gamma}\sqrt{\frac{\omega n}{\pi}}\,\mathfrak{Re}\left(\frac{1}{\tau_0} e^{-\frac{\omega\tau_0}{2\gamma^2}\frac{n}{n+1}}\right), \tag{17}$$

with $\tau_0 = e^{i\pi(1/n-1/2)}\left[2(n+1)\gamma^2 c_r\right]^{-1/n}$. Generally, it involves a power law, too, but at $n=2$ (smooth electron trajectory) the coefficient at the power-law vanishes, so the decrease becomes exponential, as described by the second term of (17).

Guessing the global behavior

Using those rules along with physically motivated values of n at $\tau \to \infty$ and $\tau \to 0$, one can assess asymptotics of the spectrum correspondingly at $\omega \to 0$ and $\omega \to \infty$. In between, the spectrum is likely to interpolate smoothly. Sometimes, the IR and UV asymptotes can cover nearly the whole spectrum (see, e.g., Fig. 5.).

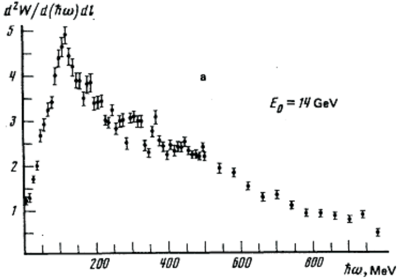

Figure: Experimental spectrum of channeling radiation from positrons in Si (110) [9].

Can n be non-integer? Computer simulation indicates that it can (cf., e.g., [10]).

Summary

- In thick targets, at $\omega \to 0$, the radiation spectrum can be highly non-dipole, but there are simple formulae at the leading and next-to-leading orders.
- At large ω, the radiation spectrum tends to be more dipole, so if it needs additional averaging, that may be safely performed by a simplified procedure.

Together, those tips can help one to promptly decipher measured radiation spectra and make direct inferences from them about the electron dynamics. However, those quick inferences ought to be subsequently checked by more rigorous numerical calculations.

References

M.V. Bondarenco,
2016, Channeling-2016, Talk on edge effects.

M.V. Bondarenco and N.F. Shul'ga,
Phys. Rev. D **95**, 056003 (2017).

F. Bloch and A. Nordsieck,
Phys. Rev. **52**, 54 (1937).

J.M. Jauch and F. Rohrlich,
Helv. Phys. Acta **27**, 613 (1954).

M.V. Bondarenco,
NLO Correction to Factorization Limit of Radiation Spectra (to be published in PRD).

F.E. Low,
Phys. Rev. **110**, 974 (1958).

L.D. Landau and I.Ya. Pomeranchuk,
Dokl. Akad. Nauk. SSSR **92**, 535 (1953).

J. Bak *et al.*,
Nucl. Phys. B **302** (1988) 525.

R.O. Avakyan, I.I. Miroshnichenko, J.J. Murray, and T. Vigut
Sov. Phys. JETP **55** (1982) 1052.

A.A. Greenenko, A.V. Chechkin, and N.F. Shul'ga,
Phys. Lett. A **324** (2004) 82-85.